

Synthesis, Spectral Characterization of Schiff Base of Some Transitional Metal Ion Complexes, Biological Activity, and Nanoparticles

Uttara M Dalvi^{1,2}, Manisha G Kapade¹, Pooja P Batawale¹ & Manohar V Lokhande^{1*}

¹Department of Chemistry, Sathaye College (Autonomous), Mumbai-400057, Maharashtra, India.

²Department of Applied Sciences, St. John Engineering College, Palghar-401404, Maharashtra, India.

Abstract:

Novel Manganese (II), Cobalt (II), Nickel (II), Copper (II), Zinc (II), and Palladium (II) Schiff metal complexes were synthesized by the condensation reaction of 4-Bromo-1,2-diaminobenzene with 4-Bromosalicylaldehyde to get the 5-bromo-2-[[[(5-bromo-2-((Z)-[(4-hydroxyphenyl) methylidene] amino) phenyl) imino] methyl] phenol. Spectral studies like FTIR (Fourier transform infrared), UV-Vis (Ultraviolet-Visible), TGA/DTA, SEM (Scanning Electron Microscope), TEM (Transmission Electron Microscope), EDX (Energy-dispersive X-ray Spectroscopy), Mass Spectra and ESR (Electron Spin Resonance), were used to characterize prepared metal complexes. The Conductance measurements, magnetic moment of complexes, and estimated metal contents have been determined and discussed. The biological properties of the synthesized compound and their complexes by antifungal, and antibacterial activity have been studied. The theoretical mass of the Prepared Schiff base is nearly equal to the prepared Schiff base. UV-Visible spectra of the complexes show, that they are colour except for Zinc (II) complexes. The parameters, such as the Nephelauxetic effect, covalence parameter $b^{1/2}$, and co-valence ($\delta\%$) are calculated. The complexes are covalent. The central metal ions have Six coordination numbers, and the ligand behaves as bidentate. The SEM, TEM, EDX, and elemental analysis of the complexes, the size of prepared nanoparticles is 38-84 nm.

Keywords: FTIR, Ultraviolet-Visible, Mass, TGA/DTA, TEM, EDX, and ESR

Introduction:

Schiff base ligands have garnered significant interest from academic researchers in recent years because of their vast variety of physicochemical properties and varied structural features. This has prompted researchers to investigate several uses for these ligands. [1–2] The structural adaptability of Schiff bases, which enables them to be used as asymmetric and stabilizing agents for a variety of complexes in varying oxidation states, is what initially sparked interest in them. [3–6] Furthermore, to control the performance of metals in a variety

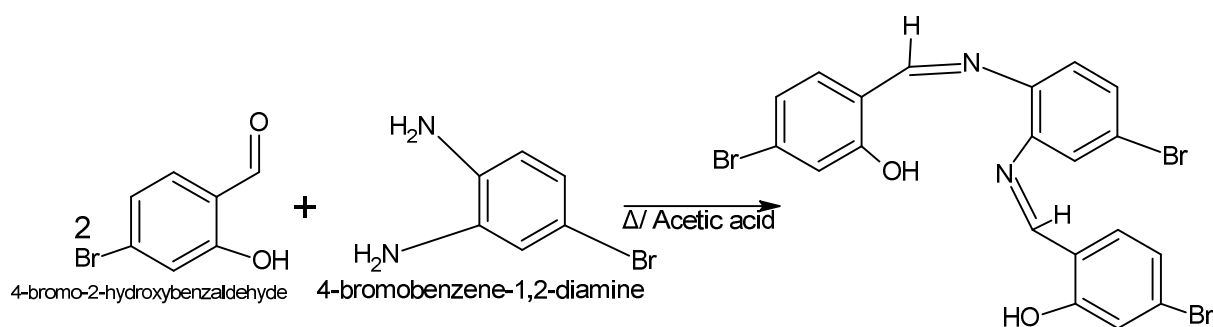
of useful transformations, Schiff bases are essential. Dinitrogen and dioxygen donor atoms facilitate the coordination of tetradentate Schiff base complexes, producing stable complexes. A few azo-azomethine metal complexes have found widespread application in technology because of their capacity for energy transfer and photophysical. Thermochromic, photochromism, electroactivity, and stability make Schiff base compounds ideal intermediates for a range of applications.[7–10] Several reviews demonstrated that the metallo-organic chemistry of these compounds has a substantial impact on their biological behaviors, emphasizing the function of metals as catalysts in a range of biological processes.[11–14] Because of the $>C=N-$ fraction planarity of their electrons, higher electronegative atoms' linked bonding orbitals, and electrons can be adsorbed on metal surfaces. The findings showed that the Schiff base metal complexes are effective corrosion inhibitors for mild steel.[15] Tetradentate Schiff base ligands and metal complexes with methoxy salicylaldehyde and substituted phenylenediamine were synthesized by Kargar and colleagues. The data show that the complexes have good catalytic activity.[16] The Schiff base compound's enhanced usefulness nowadays is largely due to its exceptional potency and ease of production of its azomethine functional group. This molecule is created by a temperature-controlled catalytic condensation reaction between an active carbonyl group and a primary amine. Although antimicrobial medicines have demonstrated efficacy in treating bacterial infections, the development of antibiotic resistance is a significant cause for concern. Therefore, using state-of-the-art methods in the design and synthesis of novel molecules is crucial. There is a great deal of activity potential in metal complexes. Schiff base ligands and their metal complexes have significant uses in the electrical, pharmacological, and biological domains, based on the activities.[17-18] Recently, screening for subsequent electronic structure-property predictions has been more efficient due to the acceleration of transition-metal chemistry discovery brought about by advancements in computational chemistry, molecular modeling, and docking.[19] In this Research Paper, a novel Schiff base ligand was created using 4-Bromo-1,2-diaminobenzene, 3-Bromosalicylaldehyde, and their complexed Mn(II), Ni(II), Co(II), Cu(II), Zn(II), and Pd(II) ions. The structural characteristics of these ligands were also examined. The ligand and complexes' antibacterial and antifungal properties.

Material and Methods:

The chemical compounds 4-bromo-1,2-diaminobenzene with 3-bromosalicylaldehyde were purchased from Sigma-Aldrich and used directly without any purification process. SD Fine Chemicals supplied metal chlorides and nitrates.

Synthesis of the Ligand:

The ligand was synthesized by refluxing an equimolar (1;1) ratio of 4-Bromo-1,2-diaminobenzene, 3-Bromosalicylaldehyde in a 75 mL ethanol solution. A few drops of glacial acetic acid were added to the reaction and refluxed by using a water condenser for two hours. After two hours, the coloured precipitate was obtained, then this precipitate was filtered, washed with hot methanol, and kept for drying at 50 °C in an Oven.



Synthesis of Metal Complexes:

The Novel Manganese (II), Cobalt (II), Nickel (II), Copper (II), Zinc (II), and Palladium (II) Schiff base metal complexes were synthesized by a 1:2 (M: L) ratio. In a round-bottom flask, 40 cm³ of Ligand 0.1M solution and 20 cm³ of Metal Chloride/Nitrate 0.01M solution were taken and vigorously stirred on a hot plate stirring Machine. The metal-ligand solution then refluxes for about three hours by adding a few drops of ethanol ammonia solution. After three hours, the solution was kept in a dark place for about eight hours, and the solid complexes were obtained. These complexes were filtered, cleaned using ethanol, and dried in vacuum desiccators. The metal complexes and ligands were soluble in DMSO and DMF solvent.

Synthesis of metal complexes nanoparticles

A metal ion solution and Schiff base ligand were mixed at an equimolar concentration of 0.01M to form the nanoparticles. After four hours of refluxing, the mixture was moved to a test tube and centrifuged for more than three hours at 6000 RPM at room temperature. The outstanding solid-coloured crystals were formed. These crystals were separated, dried, and then stored in a sealed container at room temperature. These nanoparticles were used for characterization.

Results and Discussions: The resultant ligand has a sharp melting point and is coloured, as are its tetradentate complexes. The produced compounds dissolve easily in DMSO and DMF. The calculated values for the complexes can be used to confirm the structure, and the amounts of Manganese (6.93%), Cobalt (7.39), Nickel (7.37%), Copper (7.93%), Palladium

(12.60 %), and zinc (8.148%) determined by volumetric methods and AAS used for the analysis of for Pd(II).

Equi-Tronics digital conductivity is used to evaluate molar conductance in DMSO solvent. Complexes' magnetic characteristics were examined and compared to existing literature [24-26 21–23], indicating that they had an octahedral geometrical shape. All complicated recipes have ionic neutral molar conductivity. The magnetic characteristics and molar conductivity findings for each combination are shown in Table-1. The magnetic properties of the complexes were analyzed and contrasted with previous research, revealing an octahedral geometrical structure. The molar conductivities of all the complexes are ionic neutral. The molar conductivity, physical measurements, Magnetic moment, and relative quantities of CN for MnL_2 , NiL_2 , CoL_2 , CuL_2 , PdL_2 , and ZnL_2 are given below in Table 1.

Table -1: Analytical and Physical Data (* Experimental)

Complexes/Ligand	MP/DP°C	C% *	N%*	M%*	Conductivity	μ_{eff} BM
($C_{20}H_{13}Br_3N_2O_2$)	210-213	42.19	7.57	-	-	-
[$MnC_{20}H_{11}Br_3N_2O_2 \cdot 2H_2O$]	248-251	39.39	7.07	6.93	7.2	5.20
[$Ni C_{20}H_{11}Br_3N_2O_2 \cdot 2H_2O$]	255-258	39.19	7.03	7.37	5.5	3.23
[$CoC_{20}H_{11}Br_3N_2O_2 \cdot 2H_2O$]	257-260	39.18	7.03	7.39	5.9	4.45
[$CuC_{20}H_{11}Br_3N_2O_2 \cdot 2H_2O$]	272-275	38.95	6.99	7.93	4.4	2.10
[$ZnC_{20}H_{11}Br_3N_2O_2 \cdot 2H_2O$]	280-283	38.86	6.97	8.14	4.8	0.00
[$PdC_{20}H_{11}Br_3N_2O_2 \cdot 2H_2O$]	287-290	36.98	6.63	12.60	2.0	-

Infrared Spectra of Ligand and Complexes

The infrared spectra of the ligand and the metal complexes were recorded. The infrared spectral bands of the free ligand and its metal complexes are listed in Table 2 below, along with the assignments that go with them. Due to interaction with metal ions, the ligand's $\nu(OH)$ at 3345 cm^{-1} band was visible in the ligand but not in any of the complexes. This implies that one of the phenolic-OH groups was deprotonated during the coordination phase and that the complex formation involved the phenolic-OH group. The $\nu_{HC=N}$ (imino) bond was detected in the Schiff base ligand at 1640 cm^{-1} ; however, the complexes showed this band moving between 1610 and 1620 cm^{-1} as a result of complex formation with the Schiff base and metal ions. The prominent band at 1615 cm^{-1} in the infrared spectra of the Schiff base ligand is caused by the other azomethine group $-HC=N-$ frequencies. All metal complexes have an imino group linked to metal ions in their infrared spectra. The band corresponding to $\nu(-HC=N)$ in the IR spectrum of the free ligand shifted from $1610-20\text{ cm}^{-1}$ to a lower wavenumber by $15-25\text{ cm}^{-1}$ in the IR spectra of the metal complexes, indicating the presence of the nitrogen atom in the azomethine group interacting with the metal ion [20-22]. The IR spectrum data suggests that the Schiff base ligand coordinates with the metal ions in a mono-

deprotonated form through two azomethine-N and phenolic-O centers, acting as a bidentate. The metal-ligand bonding was confirmed by the newly formed bands in the complexes' infrared spectra at 520-528 and 432-440 cm^{-1} , which were attributed to the metal-oxygen and metal-nitrogen vibrations, respectively [23-24]. Two new broad bands for coordinated water molecules are seen in IR spectra at 3430-3445 cm^{-1} and 3490-3510 cm^{-1} [25].

Table 2: FTIR of Schiff base ligand and metal complexes

L/Complexes	νOH	$\nu\text{HC=N}$	$\nu\text{H}_2\text{O}$	$\nu\text{H}_2\text{O}$	$\nu\text{HC=N}$	$\nu\text{M-O}$	$\nu\text{M-N}$
($\text{C}_{20}\text{H}_{13}\text{Br}_3\text{N}_2\text{O}_2$)	3345	1615	-	-	1640	-	-
[$\text{MnC}_{20}\text{H}_{11}\text{Br}_3\text{N}_2\text{O}_2 \cdot 2\text{H}_2\text{O}$]	-	1602	3445	3498	1630	522	438
[$\text{Ni C}_{20}\text{H}_{11}\text{Br}_3\text{N}_2\text{O}_2 \cdot 2\text{H}_2\text{O}$]	-	1605	3440	3494	1624	520	434
[$\text{CoC}_{20}\text{H}_{11}\text{Br}_3\text{N}_2\text{O}_2 \cdot 2\text{H}_2\text{O}$]	-	1610	3430	3490	1628	522	432
[$\text{CuC}_{20}\text{H}_{11}\text{Br}_3\text{N}_2\text{O}_2 \cdot 2\text{H}_2\text{O}$]	-	1604	3438	3504	1625	528	435
[$\text{ZnC}_{20}\text{H}_{11}\text{Br}_3\text{N}_2\text{O}_2 \cdot 2\text{H}_2\text{O}$]	-	1601	3440	3510	1627	523	440

Electronic Spectra and Magnetic Susceptibility: The Bohr magneton (BM) is a unit used to measure the strength of an electron's magnetic field. The magnetic moment of an ion is calculated using the formula $\mu=n(n+2)$ BM, where 'n' is the number of unpaired electrons. The presence of unpaired electrons in an ion makes it paramagnetic, which attracts it to a magnetic field. The first transition series of elements includes transition metals that form coloured ions and compounds. The magnetic moment values (B.M.) and electronic spectrum data for the Mn (II), Co (II), Ni (II), and Cu (II) complexes are shown in Table 3. At ambient temperature, the electronic absorption spectra and magnetic moments of the metal complexes under investigation were measured in DMSO (10^{-3} M). The electronic spectra of the Mn (II) complex showed one absorption band at 581 nm because of the ${}^6\text{A}_{1g} \rightarrow {}^4\text{T}_{2g}(\text{G})$ transition in an octahedral shape. The magnetic moment value of 5.20 B.M. for the Mn(II) complex verified its octahedral geometry[26]. The Co (II) complex showed a characteristic band at 575 nm, which could be related to the octahedral ${}^4\text{T}_{1g}(\text{F}) - {}^4\text{A}_{2g}(\text{F})$ transition. Three unpaired electrons in an octahedral configuration were suggested by the magnetic moment value of 4.45 B.M [37]. In an octahedral stereochemistry, the Ni (II) complex electronic spectra showed three bands at 455,530 and 650 nm that correlated to the $d \ {}^3\text{A}_{2g} \rightarrow {}^3\text{T}_{2g}$, ${}^3\text{A}_{2g}(\text{F}) \rightarrow {}^3\text{T}_{1g}(\text{F})$, and ${}^3\text{A}_{2g}(\text{F}) \rightarrow {}^3\text{T}_{1g}(\text{P})$ transitions, respectively. The magnetic moment value indicates the octahedral geometry surrounding the Ni (II) ion, which is 3.23 B.M [28]. Two bands at 605 and 660 nm in the Cu (II) complex's electronic spectra are ascribed to the ${}^2\text{B}_{1g} - {}^2\text{E}_g$ and ${}^2\text{B}_{1g} - {}^2\text{B}_{2g}$ transitions, respectively. One unpaired electron in an octahedral structure is indicated by the magnetic moment value of 2.10 B.M [29]. It was discovered that the current Cu (II) complex has a relatively high magnetic moment value of 2.04 B.M. This observation implies a spin-spin ferromagnetic coupling interaction, where the magnetic

moment value is higher than expected because the spins of the two unpaired electrons in the two adjacent Cu (II) ions are in the same direction and their moments are parallel to one another. Zn (II) is a colourless solution and is diamagnetic.

Table 3 : Electronic Spectra and Their Parameter

Complexes	Bands (nm)	β	1- β	η	$b^{1/2}$	$\delta\%$
[Ni C ₂₀ H ₁₁ Br ₃ N ₂ O ₂ .2H ₂ O]	455,530,650	0.9650	0.0350	0.0180	0.0935	1.8341
[CoC ₂₀ H ₁₁ Br ₃ N ₂ O ₂ .2H ₂ O]	575	0.9755	0.0245	0.0127	0.0790	1.2711
[CuC ₂₀ H ₁₁ Br ₃ N ₂ O ₂ .2H ₂ O]	605,660	0.9730	0.0270	0.0137	0.0821	1.3771

Electron Spin Resonance spectra

Powdered Co(II) and Cu(II) complexes' ESR spectra were captured at ambient temperature. The hyperfine interaction with the nuclear spin of ⁵⁹Co caused the Co(II) complex's ESR spectrum to show a single signal split into eight lines. The Co(II) complex has a g_{aff} - value of 2.0122. The covalent nature of the link between the Co(II) ion and the ligand is suggested by the positive departure from the free electron value (2.0022) [30]. Two signals with two distinct g-values, 2.109 and 2.049 for g_{\parallel} and g_{\perp} , respectively, and $g_{\text{av}} = 2.089$ are visible in the Cu (II) complex's X-band ESR spectrum. The analyzed Cu (II) complex has an octahedral geometry, according to the form of the ESR spectrum with the g-tensor values [31]. $g_{\parallel} > g_{\perp} > 2.0023$, indicating that the unpaired electron is located in the dx^2-y^2 orbital, resulting in the ground state being $^2B^1_g$ [32]. The covalent character of the Cu-L bond is shown by a g_{\parallel} value < 2.3 [33]. The formula for calculating the exchange interaction term (G) is $G = (g_{\parallel} - 2.0023)/(g_{\perp} - 2.0023)$. If $G > 4.0$, the local tetragonal axes are parallel or slightly misaligned, but if $G < 4.042$, there is a considerable exchange coupling and misalignment. The exchange coupling effects between Cu (II) centers were active in the current Cu (II) complex43, as shown by the calculated G-value of 1.94 for the Cu (II) complex.

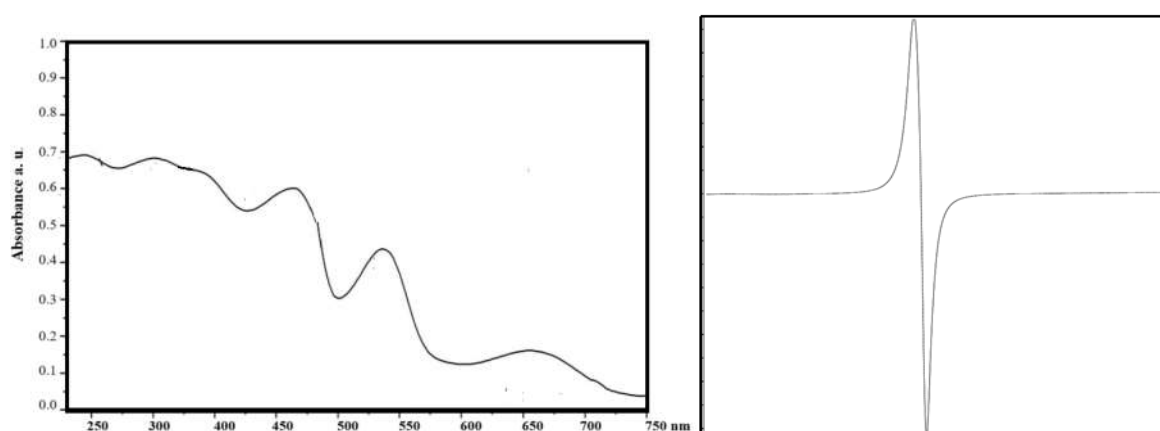


Figure 1: (A) UV-VIS of Ni(II) Complex , B) ESR of Co(II) Complex

SEM, TEM and EDX: The complexes' SEM, TEM, and EDX micrographs are displayed beneath the pictures. These molecules' SEM and TEM pictures show a granular arrangement

with a spherical structure [34-35]. The produced complexes had particle sizes ranging from 38-84 nm. The complex contains corrected components found in prepared complexes, according to EDX analysis.

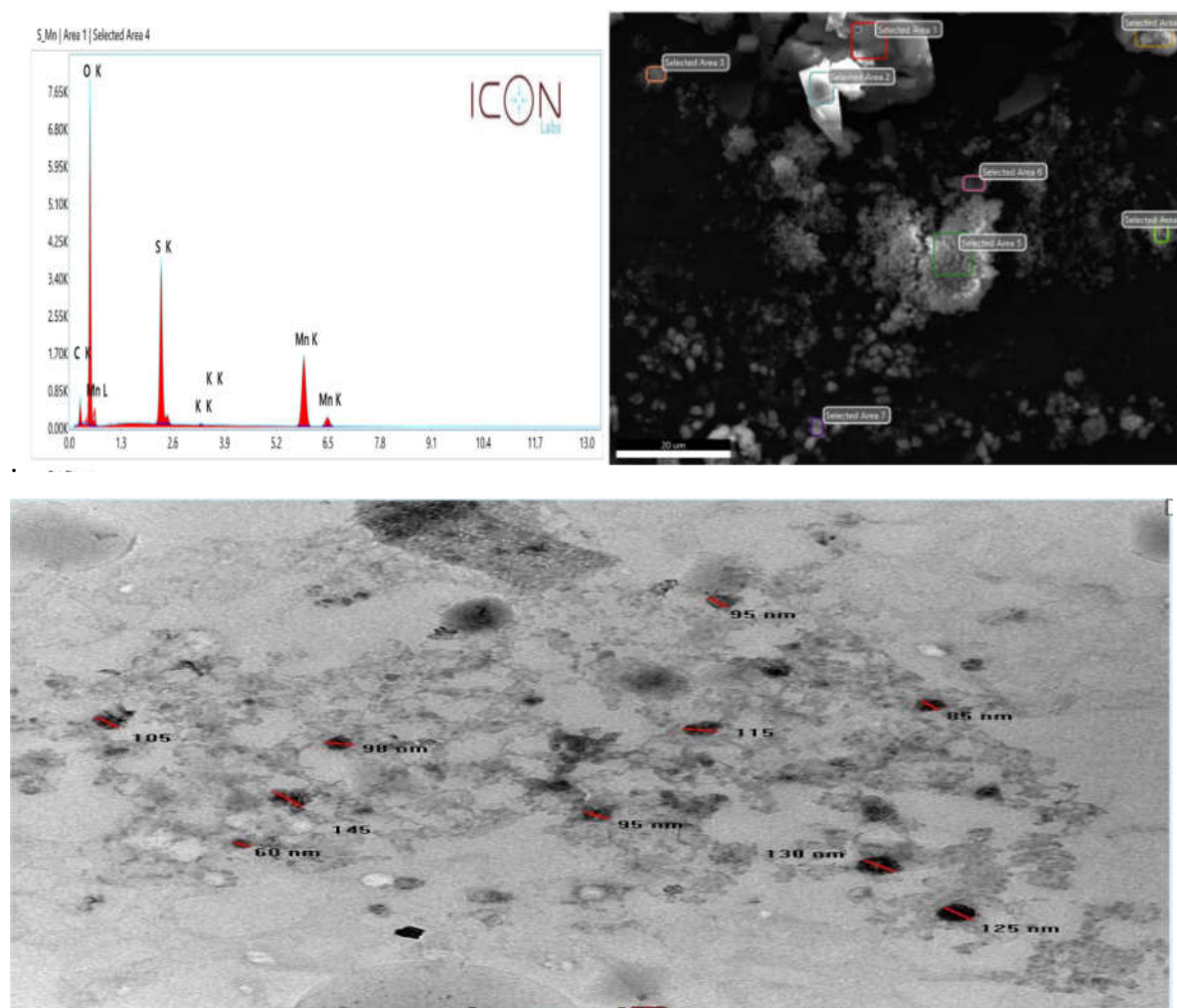


Figure 2: EDX, SEM, and TEM of Mn (II) Complex

Thermal analysis:

Thermogravimetric and differential thermal analysis results of $[\text{NiC}_{20}\text{H}_{11}\text{Br}_3\text{N}_2\text{O}_2 \cdot 2\text{H}_2\text{O}]$ and $[\text{PtC}_{20}\text{H}_{11}\text{Br}_3\text{N}_2\text{O}_2 \cdot 2\text{H}_2\text{O}]$ are reported. These complexes are thermally stable at room temperature and decompose in different stages. Complexes lose weight due to exothermic and endothermic processes [36].

$[\text{NiC}_{20}\text{H}_{11}\text{Br}_3\text{N}_2\text{O}_2 \cdot 2\text{H}_2\text{O}]$ complex:

Two coordinated water molecules and some portion of the chelate are lost in the temperature range of 30 to 195°C, according to a thermal analysis study of the Ni^{2+} complex. The TGA analytical curve yields an experimental percentage loss of 14.15. The theoretical % loss value and this amount are comparable. At this range, the differential thermal analysis peak is endothermic. The complex is mostly lost at temperatures between 250 and 520°C. The

Thermo gravimetric analysis curve yields the experimental percentage loss, which is 23.15. The theoretical % loss values and the experimental percentage loss value are comparable. The Figure shows that the differential thermal analysis peak is exothermic. Finally, we get the metal oxide in the temperature range 700 to 900°C.

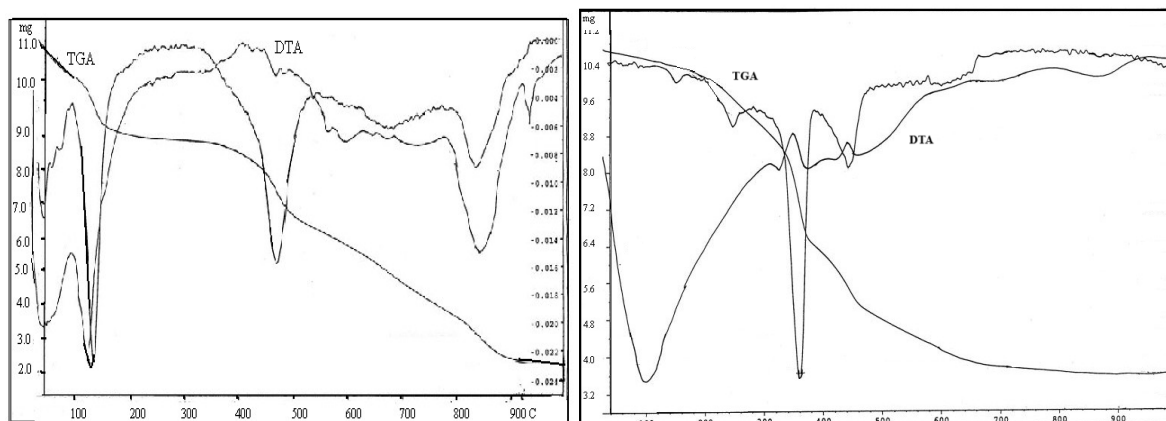


Figure-3: TGA/ DTA of $[\text{NiC}_{20}\text{H}_{11}\text{Br}_3\text{N}_2\text{O}_2 \cdot 2\text{H}_2\text{O}]$ & $[\text{PtC}_{20}\text{H}_{11}\text{Br}_3\text{N}_2\text{O}_2 \cdot 2\text{H}_2\text{O}]$ complex:

Pt^{2+} complex weight loss occurs in four stages, according to thermal analysis. Two coordinated water molecules and some portions of the complex are lost in the first stage, which occurs at temperatures between 30 to 190°C. Based on the TG curve, the experimental percentage loss is 14.28. The DTA peak at this range is endothermic, and it is comparable to the theoretical % loss amount. A portion of the complex is lost in the second stage, which occurs at temperatures between 190 to 310°C. The likely leaving groups are $\text{C}_6\text{H}_4\text{NBr}$. The majority of a chelating agent is lost in the third stage between 320 to 490 degrees Celsius. The TGA curve yields the experimental percentage loss of 22.98. The theoretical percentage loss value of 23.10 is comparable to the experimental percentage loss value. Exothermic is the apex of the differential thermal analysis. Most of the portion of ligand that was lost is the most likely remaining component of a complex in this temperature range. Platinum oxide is formed in the last stage at temperatures between 510 to 900 degrees Celsius.

Mass Spectra of Schiff Base and Complexes:

At room temperature mass spectra of the ligands and metal complexes are listed in the below table. The Cu (II) complex has a theoretical mass of $m/z = 650.60$. In a similar vein, the molecular weight of the Zn (II) complex is $m/z = 652.44$, but the molecular peaks of the Cu (II) and Zn (II) complexes appear at $m/z = 651.48$ and 653.48 , respectively, which correspond to $[\text{M}+1]$. The complexes' structure is supported by these summits. The various molecular ion peaks that emerged in complex mass spectra are explained by the metal complex molecule's

fragmentation, which was caused by the breaking of several internal bonds and subsequent degradation that produced numerous additional significant peaks as a result of the production of different radicals.

Table-4: Mass spectra of the Schiff bases and complexes

Ligand/Complex	Expected m/z	Found m/z	Peak assigned
(C ₂₀ H ₁₃ Br ₃ N ₂ O ₂)	553.04	552.97	M
[MnC ₂₀ H ₁₁ Br ₃ N ₂ O ₂ .2H ₂ O]	642.00	641.94	M
[Ni C ₂₀ H ₁₁ Br ₃ N ₂ O ₂ .2H ₂ O]	645.75	645.45	M
[CoC ₂₀ H ₁₁ Br ₃ N ₂ O ₂ .2H ₂ O]	645.99	645.95	M
[CuC ₂₀ H ₁₁ Br ₃ N ₂ O ₂ .2H ₂ O]	650.60	651.48	M+1
[ZnC ₂₀ H ₁₁ Br ₃ N ₂ O ₂ .2H ₂ O]	652.44	653.48	M+1

Microbial activity

Using the agar gel diffusion method, the preparation of Schiff Base and its metal (II) complexes were tested in vitro for their antibacterial activity against two strains of Gram-positive bacteria, *B subtilis* and *S aureus*, and two strains of Gram-negative bacteria, *S flexenari* and *P aeruginosa* [37]. The plates were incubated for 24 hours at 37°C right away. The diameter of the zones exhibiting total inhibition (mm) was used to calculate activity. The conventional medication and growth inhibitions were contrasted [38]. Separate tests using DMSO solutions alone were conducted to elucidate any potential involvement of DMSO in biological screening; however, they demonstrated no activity against any bacterial strains. The results were recorded as zones of inhibition in mm and were compared with standard drugs.

Table 5: Microbial activity

	B subtilis	S aureus	S flexenari	P aeruginosa
(C ₂₀ H ₁₃ Br ₃ N ₂ O ₂)	14	16	12	12
[MnC ₂₀ H ₁₁ Br ₃ N ₂ O ₂ .2H ₂ O]	16	20	14	14
[Ni C ₂₀ H ₁₁ Br ₃ N ₂ O ₂ .2H ₂ O]	18	18	16	16
[CoC ₂₀ H ₁₁ Br ₃ N ₂ O ₂ .2H ₂ O]	19	21	17	17
[CuC ₂₀ H ₁₁ Br ₃ N ₂ O ₂ .2H ₂ O]	21	23	19	17
[ZnC ₂₀ H ₁₁ Br ₃ N ₂ O ₂ .2H ₂ O]	23	22	20	18
[PtC ₂₀ H ₁₁ Br ₃ N ₂ O ₂ .2H ₂ O]	24	22	19	21

(10 & less: very weak; 10 & above: weak; 15 & above good; 20 & above: very good)

Conclusions

Schiff base has been synthesized, along with its metal complexes of Mn (II), Co (II), Ni (II), Cu (II), Zn (II), and Pt (II). These complexes were characterized by various spectral analyses, it was discovered that each one had a metal-ligand stoichiometry of 1:1. All of the complexes are naturally non-electrolytes. Through the nitrogen atom of the anilino and the oxygen atoms of the hydroxyl group of the 5-bromo-2-[(5-bromo-2-[(Z)-[(4-bromo-hydroxyphenyl)

methylidene] amino} phenyl) imino] methyl} phenol, the ligand functions as a neutral and monodentate coordinating agent, according to the spectrum data. All of these complexes are classified as having an octahedral geometry based on spectral, magnetic, molar conductance, and analytical data. The size of prepared NPs is between 38 to 84 nm. Additionally, antimicrobial studies show that the metal complexes are more effective antibacterial agents than Schiff bases.

Acknowledgment:

The authors are thankful to the Principal and Department of Chemistry, Sathaye College, for providing the necessary Research Laboratory Facilities. ICON Labs provides SEM, TEM and EDX facilities.

Declaration of Competing Interest:

The authors declare that they have no known competing financial interests or personal relationships that could have appeared to influence the work reported in this paper.

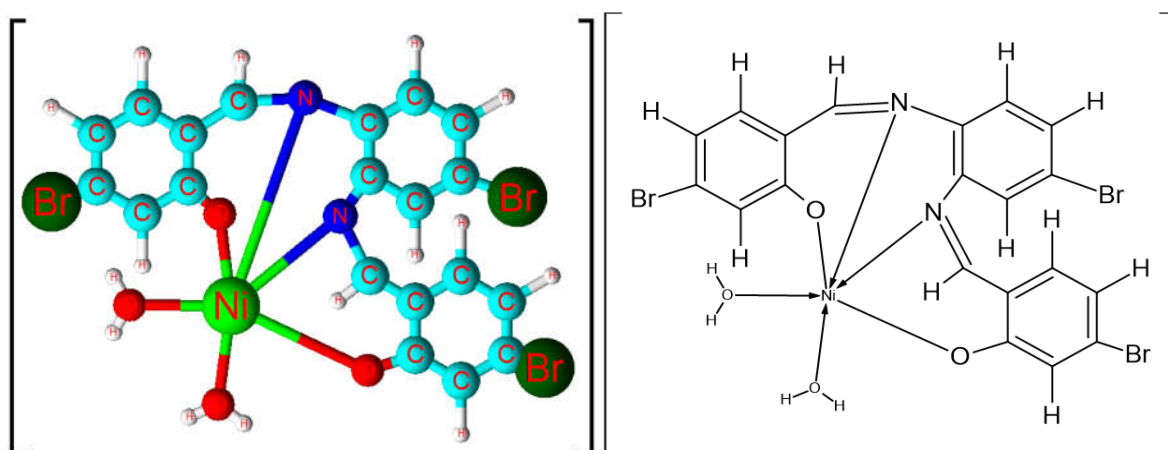


Figure -4: Structure of Complex

References :

1. Chen L, Wang L, An W, Wang R, Tian L. Synthesis, structural characterization, and antibacterial activity of diorganotin complexes of Schiff base derived from 4-(diethylamino)- salicylaldehyde and L-tyrosine. *Inorganic Nano-Material Chemistry*. 2020; 50 (9): 872–879. <https://doi.org/10.1080/24701556.2020.1727515>.
2. Kaushik S, Paliwal SK, Iyer MR, Patil VM. Promising Schiff bases in antiviral drug design and discovery. *Medical Chemistry Research*, 2023; 32: 1063–1076. <https://doi.org/10.1007/s00044-023-03068-0>.
3. Muthukkumar M, Kamal C, Venkatesh G, Kaya C, Kaya S, Enoch IVMV, Vennila P, Rajavel R. Structural, spectral, DFT and biological studies on macrocyclic

- mononuclear ruthenium (II) complexes. *Journal of Molecular Structure*. 2017; 1147: 502–514. <https://doi.org/10.1016/j.molstruc.2017.06.132>.
4. Putaya AN, Ndahi NP, Bello HS, Mala G, Osunlaja AA, Garba H, Synthesis, characterization and antimicrobial analysis of Schiff bases of o-phenylenediamine and 2-aminopyridine-3-carboxylic acid with ofloxacin and their metal (II) complexes. *International Journal of Biological and Chemical Sciences*. 2020; 14(1): 263-278. <https://doi.org/10.4314/ijbcs.v14i1.22>.
 5. Verma R, Lamba NP, Dandia A, Srivastava A, Modi K, Chauhan MS, Prasad J. Synthesis of N Benzylideneaniline by Schiff base reaction using Kinnow peel powder as Green catalyst and comparative study of derivatives through ANOVA techniques. *Scientific Reports*. 2022; 12: 9636. <https://doi.org/10.1038/s41598-022-13360-5>.
 6. Maleki A, Hajizadeh Z, Salehi P. Mesoporous halloysite nanotubes modified by CuFe₂O₄ spinel ferrite nanoparticles and study of its application as a novel and efficient heterogeneous catalyst in the synthesis of pyrazole pyridine derivatives. *Scientific Reports*, 2019; 9(1): 1–8. <https://doi.org/10.1038/s41598-019-42126-9>.
 7. Hajizadeh Z, Radinekiyan F, Eivazzadeh R, Maleki A. Development of novel and green NiFe₂O₄ geopolymer nanocatalyst based on bentonite for the synthesis of imidazole heterocycles by ultrasonic irradiations. *Scientific Reports*. 2020; 10(1):1-11. <https://doi.org/10.1038/s41598-020-68426-z>.
 8. Dasari RR, Haranath C, Ahad HB. Complex Drug Delivery Systems. *International Journal of Pharmaceutical Science and Research*. 2022; 13(4): 1533-1539. [https://doi.org/10.13040/IJPSR.0975-8232.13\(4\).1533-39](https://doi.org/10.13040/IJPSR.0975-8232.13(4).1533-39).
 9. Choudhary MR, Lokhande MV. Some transitional metal ions complexes with 3-[(e)-(4-fluorophenyl) methylidene] amino} benzoic acid and its microbial activity. *International Journal of Pharmaceutical Science and Research*. 2014; 5(5): 1757-1766. [https://doi.org/10.13040/IJPSR.0975-8232.5\(5\).1757-66](https://doi.org/10.13040/IJPSR.0975-8232.5(5).1757-66).
 10. Lokhande MV, Gulam FM. Spectral Studies of Some Transition Metal Ion Complexes with 4[(E)-(Ferrocene-1-Methylidene) Amino] Pyridin-2-ol. *Journal of Applied Chemistry*. 2014; 6(6): 36-42. <https://doi.org/10.9790/5736-0663642>.
 11. Ravula MR. Synthesis, characterization, and antimicrobial activity of Schiff base ligand and Metal complexes. *Indian Journal of Chemistry*. 2024; 63(3): 281-285. <https://doi.org/10.56042/ijc.v63i3.6539>.

12. George AA, Lokhande MV. Spectral Studies of New Organometallic Schiff Base Complexes and their Anti-Fungal Activity. *International Journal of Pharmaceutical Science and Research*. 2017; 8(8): 3413-3420. [https://doi.org/10.13040/IJPSR.0975-8232.8\(8\).3413-20](https://doi.org/10.13040/IJPSR.0975-8232.8(8).3413-20).
13. Drosou M, Mitsopoulou CA, Orio M, Pantazis DA. EPR Spectroscopy of Cu(II) Complexes: Prediction of g-Tensors Using Double-Hybrid Density Functional Theory. *Magnetochemistry*. 2022; 8: 36. <https://doi.org/10.3390/magnetochemistry8040036>.
14. Wazir I, Ndhahi NP, Paul BB. Synthesis, Physicochemical and Antimicrobial Studies of Co(II), Zn(II) and Fe(III) Mixed Antibiotics Metal Complexes. *Journal of Chemical and Pharmaceutical Research*. 2013; 5(9): 84-89.
15. Kapade MG, Batawale PP, Raut UM, Lokhande MV. Synthesis, Characterization Of 2-[(Z)-{[6-Amino-2-(4-Chlorophenyl) Pyrimidin-4-Yl] Imino} Methyl]-4-Nitrophenol Schiff Base With Mn (II), Co (II), Ni (II), Cu(II), Zn (II), Pt (II) for their Nanoparticle and Antibacterial Studies. *Rasayan Journal of Chemistry*. 2024; 17(4): 1426-1435. <http://doi.org/10.31788/RJC.2024.1748925>.
16. Boulechfar C, Ferkous H, Delimi A, Djedouani A, Kahlouche A, Boubliia A, Darwish AS, Lemaoui T, Verma R. Schiff bases and their metal Complexes: A review on the history, synthesis, and applications. *Inorganic Chemistry Communication*. 2023, 150, 110451. <https://doi.org/10.1016/j.inoche.2023.110451>.
17. Venkatesh G, Vennila P, Kaya S, Ahmed SB, Sumathi P, Siva V, Rajendran PK, Kamal C. .Synthesis and Spectroscopic Characterization of Schiff Base Metal Complexes, Biological Activity, and Molecular Docking Studies. *ACS Omega*. 2024; 9(7): 8123–8138. <https://doi.org/10.1021/acsomega.3c08526>.
18. Yusuf TL, Oladipo SD, Zamisa S, Kumalo HM, Lawal IA, Lawal MM, Mabuba N. Design of new Schiff-Base Copper (II) complexes: Synthesis, crystal structures, DFT study, and binding potency toward cytochrome P450 3A4. *ACS Omega* **2021**, 6, 13704– 13718, <https://doi.org/10.1021/acsomega.1c00906>.
19. Muthu S, Ramachandran G. Spectroscopic studies (FTIR, FT-Raman and UV–Visible), normal coordinate analysis, NBO analysis, first-order hyper polarizability, HOMO and LUMO analysis of (1R)-N-(Prop-2-yn-1-yl)-2,3-dihydro-1H-inden-1-amine molecule by ab initio HF and density functional methods. *Spectrochimica Acta Part A: Molecular and Biomolecular Spectroscopy*. 2014; 121: 394– 403. <https://doi.org/10.1016/j.saa.2013.10.093>.

20. Kapade MG, Batawale PP, Dalvi UM, Lokhande MV. Synthesis and Characterization of Noval Schiff Base Complexes of Mn(II), Co(II), Ni(II), Cu(II), Zn(II), Pd(II), Pt(II) Metal Ions for Microbial Activities and Their Nanoparticles. *International Journal of Pharmaceutical Sciences and Research*. 2024;15(11): 3297-3306. [https://doi.org/10.13040/IJPSR.0975-8232.15\(11\).3297-06](https://doi.org/10.13040/IJPSR.0975-8232.15(11).3297-06).
21. Gulam FM, Lokhande MV. Electronic Spectra, Thermal Analysis, X-Ray Powder Diffraction, and SEM Studies of Organometallic Compound. *International Journal of Scientific Research*. 2013; 4(12): 457-460. <https://doi.org/10.36106/IJSR>.
22. Adly OMI, Shebl M, Abdelrhman EM, El-Shetary BA. Synthesis, spectroscopic, X-ray diffraction, antimicrobial and antitumor studies of Ni(II) and Co(II) complexes derived from 4-acetyl-5,6-diphenyl-3(2H)-pyridazinone and ethylenediamine. *Journal of Molecular Structure*. 2020; 1219: 128607. <https://doi.org/10.1016/j.molstruc.2020.128607>.
23. Aravindan P, Sivaraj K, Kamal C, Vennila P, Venkatesh G. Synthesis, Molecular structure, Spectral Characterization, Molecular docking and biological activities of (E)-N-(2-methoxy benzylidene) anthracene-2-amine and Co(II), Cu(II) and Zn(II) complexes. *Journal of Molecular Structure*. 2021;1229:129488. <https://doi.org/10.1016/j.molstruc.2020.129488>.
24. Patil SA, Prabhakara CT, Halasangi BH, Toragalmath SS, Badami PS, DNA cleavage, antibacterial, antifungal and anthelmintic studies of Co(II), Ni(II) and Cu(II) complexes of coumarin Schiff bases: Synthesis and spectral approach. *Spectrochimica Acta Part A: Molecular and Biomolecular Spectroscopy*. 2015;137: 641-651. <https://doi.org/10.1016/j.saa.2014.08.028>.
25. Salehi M, Rahimifar F, Kubicki M, Asadi A. Structural, spectroscopic, electrochemical and antibacterial studies of some new nickel(II) Schiff base complexes. *Inorganica Chimica Acta*. 2016;443:28-35. <https://doi.org/10.1016/j.ica.2015.12.016>.
26. Handley RC. Modern magnetic materials: principles and applications(. John Wiley & Sons.2010, 83.
27. Johnson RC, Basolo F. Coordination Chemistry: The Chemistry of Metal Complexes(W. A. Benjamin, Inc. 1964.
28. Cotton FA, Wilkinson G. Advanced Inorganic Chemistry, Wiley,NY, 5th Ed.,1988.
29. Gulam FM, Lokhande MV. Some Transitional Metal Ion Complexes With 2,2'-{1,1'-Bi(Ferrocene-2,4-Dien-1-yl) -2,2'-Diylbis[Nitrilo(E) Methylidene]} Bis (4-

- Chlorophenol) and Antimicrobial Activity. *Journal of Applicable Chemistry*.2013;2(6):1711-1720.
30. Mishra A, Mishra R, Shrivastavaap S. Structural and antimicrobial studies of coordination compounds Of VO (II), Co (II), Ni (II) and Cu (II) with some Schiff bases involving 2-amino-4-chlorophenol. *Journal of Serbian Chemical Society*. 2009; 74 (5): 523–535.
31. Ding B, Yi L, Zheng S, Cheng P, Zheng LD, Ping Y, Jiang ZH. Synthesis, crystal structure, and magnetic properties of N1, N2-bridged polynuclear Ni(II) complexes. *Journal of Molecular Structure*. 2006, 1(3): 138–143.
32. Figgis B. Introduction to Ligand Field, Wiley Eastern Ltd., New Delhi, 2005.
33. Carlin R, Van Dryneveled A., Magnetic Properties of Transition Metal Compounds, Springer Verlag, New York,1997.: Lever ABP. Inorganic Electronics Spectroscopy, Elsevier Amsterdam, 1968.
34. Lokhande MV, Kokate PR, Sapkale KM, Tembulkar M. Bio-Synthesis of AgNPs and MnNPs of Philodendron giganteum Herbal Extract and catalysis's activity. *Asian Journal of Research in Pharmaceutical Sciences*. 2024;14(2):122-128. <https://doi.org/10.52711/2231-5659.2024.00018>.
35. Verma AS, Blessyhyrose B, Gupta VS, Kokate PR, Lokhande MV. Biosynthesis of AgNPs and CuNPs from plant extract of Gymnema Sylvestre. *Degrees Journal*. 2024;9(11):75-82. <https://doi.org/12.1789001.DEJ.2024.V9I11.24.411876>.
36. Shivankar VS, Vaidya RB, Dharwadkar SR, Thakkar NV. Synthesis, characterization, and biological activity of mixed ligand Co(II) complexes of 8-Hydroxyquinoline and some amino acids. *Synthesis and Reactivity in Inorganic and Metal-Organic Chemistry*, 2003; 33(9): 1597-1622.
37. Rosato A, Catalano A, Carocci A, Carrieri A, Carone A, Caggiano G, Franchini C, Corbo F, Montagna MT. In vitro interactions between anidulafungin and nonsteroidal anti-inflammatory drugs on biofilms of Candida spp. *Bioorganic Medicinal Chemistry*. 2016;24:1002–1005. <https://doi.org/10.1016/j.bmc.2016.01.026>.
38. Hassan AS, Askar AA, Nossier ES, Naglah AM, Moustafa GO, Al-Omar MA. Antibacterial evaluation, in silico characters, and molecular docking of Schiff bases derived from 5-aminopyrazoles. *Molecules*. 2019;24:3130. <https://doi.org/10.3390/molecules24173130>.